Physics Letters A 375 (2011) 3677–3681

Contents lists available at SciVerse ScienceDirect

Physics Letters A

www.elsevier.com/locate/pla

Dynamics of unidirectionally coupled bistable Hénon maps

J.M. Sausedo-Solorio [a], A.N. Pisarchik [b,*]

[a] Advanced Physics Laboratory, Universidad Autonoma del Estado de Hidalgo, Carretera Pachuca-Tulancingo 1000, Pachuca, Hidalgo, Mexico
[b] Centro de Investigaciones en Optica, Loma del Bosque 115, Lomas del Campestre, Leon, Guanajuato, Mexico

ARTICLE INFO

Article history:
Received 17 May 2011
Received in revised form 25 July 2011
Accepted 30 July 2011
Available online 26 August 2011
Communicated by A.R. Bishop

ABSTRACT

We study dynamics of two bistable Hénon maps coupled in a master-slave configuration. In the case of coexistence of two periodic orbits, the slave map evolves into the master map state after transients, which duration determines synchronization time and obeys a $-1/2$ power law with respect to the coupling strength. This scaling law is almost independent of the map parameter. In the case of coexistence of chaotic and periodic attractors, very complex dynamics is observed, including the emergence of new attractors as the coupling strength is increased. The attractor of the master map always exists in the slave map independently of the coupling strength. For a high coupling strength, complete synchronization can be achieved only for the attractor similar to that of the master map.

1. Introduction

Multistability is a phenomenon in a dissipative system when several stable states coexist for a given set of system parameters. This phenomenon was observed in many fields of science, including electronics [1], optics [2], mechanics [3], and biology [4]. Among many mechanisms responsible for the emergence of multistability, we find homoclinic tangencies in weakly dissipative systems, increasing complexity in coupled nonlinear systems, delayed feedback, and uncertain destination dynamics. In spite of different origin of multistability, the overall behavior of multistable systems is rather similar. All they are characterized by extremely high sensitivity to initial conditions; very small perturbations may already cause a change in the final state. Furthermore, the qualitative behavior of the system changes often drastically under a very small variation of a system parameter; the intervals of the coexistence of attractors can be rather small so that a slight perturbation in a control parameter may cause a rapid change in the number of coexisting attractors giving rise to a very complex dynamics.

One of the simplest ways to construct a multistable system is to take a conservative system and add a small amount of dissipation. This way the island of a marginal stable motion in the conservative system turns into attractors. For a sufficiently small dissipation, many coexisting attractors emerge, they are mainly low-periodic orbits as it has been shown for the single and double rotor, the Hénon map, and the optical cavity map [5–7]. Multistability can appear in coupled systems due to increasing complexity [8,9]. Most studies performed so far had dealt with dynamical systems which being uncoupled were monostable, with some notable exceptions [10–13]. For example, Yanchuk and Kapitaniak [9] considered two identical Rössler systems and observed coexistence of chaotic attractors induced by weak mutual coupling. Multistability in mutually coupled Hénon maps and neuron maps has been studied by Astakhov et al. [14,15]. Synchronization of two mutually coupled bistable chaotic Lorenz systems with negative feedback has been studied by Kapitaniak [16]. He found that the final attractor of the synchronized state strongly depends on the actual position of trajectories on their attractors in the moment when coupling is introduced. Synchronization of bistable systems coupled in a master–slave configuration has been studied using chaotic Rössler oscillators [10–12]. This coupled system displays a very rich dynamics including different types of synchronization, intermittency, shift of natural oscillator frequencies, frequency locking, etc. Similar problem has been considered in a bistable semiconductor laser subject to the injection of the radiation from another identical laser [13]. In continuous time systems, one deals with differential equations, where for a very strong coupling the master system becomes monostable and complete synchronization is always achieved.

In this work we study complex dynamics of two bistable discrete systems coupled in a master–slave configuration, namely, we choose the Hénon map as a paradigm system which exhibits the coexistence of attractors. Therefore, the results obtained with the Hénon map may be generalized to a wide class of multistable systems, taking into account that an iterative map can be interpreted as a Poincare section of a continuous system. The principal difference in synchronization of continuous and discrete systems occurs for a very strong coupling, when the contribution of the coupling variable of the master system dominates over the corresponding variable of the slave system. We will show that even for a

* Corresponding author.
E-mail address: apisarch@cio.mx (A.N. Pisarchik).

0375-9601/$ – see front matter
doi:10.1016/j.physleta.2011.07.057

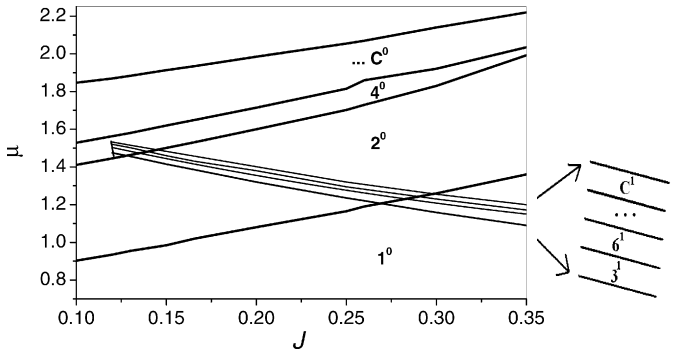

Fig. 1. State diagram of the Hénon map Eq. (1) in the (J,μ)-parameter space. 1^0, 2^0, 4^0, C^0 and 3^1, 6^1, C^1 indicate, respectively, period 1, 2, 4, and chaos and period 3, 6, and another chaotic state. The bistability region exists for $1.1 \lesssim \mu \lesssim 1.6$.

very strong coupling, while the similar attractor exists in the slave map as in the master map, another attractor also presents, i.e. the slave subsystem remains bistable. Complete synchronization can be achieved only when the master and the slave maps stay in similar attractors.

The rest of the Letter is organized as follows. In Section 2 we show how multistability emerges in the Hénon map and present the fixed points analysis of the system of two unidirectionally coupled identical Hénon maps. Sections 3 and 4 are devoted to a study of synchronization of the Hénon maps with two coexisting periodic orbits and with coexistence of a limit cycle and chaos. Finally, the main conclusions are given in Section 4.

2. Multistable Hénon map

The Hénon map [17] is a classical example of a two-dimensional multistable system:

$$x_{n+1} = 1 - \mu x_n^2 + y_n,$$
$$y_{n+1} = -J x_n. \tag{1}$$

By varying the parameters μ and J it is possible to find regions where different attractors coexist, as shown in Fig. 1. Two intersected cascades of period-doubling bifurcations terminated in chaos are presented in the figure; one cascade starts from the period 1 (denoted by super-index 0) and another cascade starts from the period 3 (denoted by super-index 1). The period-doubling bifurcation lines separate different periodic regimes. The coexistence of two different attractors can be found within the intervals of $\mu \in [1.1, 1.6]$ for $J > 0.12$.

For definiteness, in this work we fix the parameter $J = 0.166$ and vary the parameter μ to explore the coexistence of the period 2^0 with the period 3^1 and the period 2^0 with chaos C^1. The bifurcation diagram of the variable x with μ as a control parameter is shown in Fig. 2.

2.1. Two unidirectionally coupled Hénon maps

Using the difference coupling via variable y, the slave map dynamics is described as follows

$$u_{n+1} = 1 - \mu u^2 + v_n + \varepsilon(y_n - v_n),$$
$$v_{n+1} = -J u_n, \tag{2}$$

where u and v are the state variables of the slave map and $\varepsilon \in [0,1]$ is the coupling strength. Note, that the master map dynamics is guided by Eq. (1).

Fig. 3 shows the state diagram of the coupled system in the (ε,μ)-parameter space. The coupling strength gives rise in new

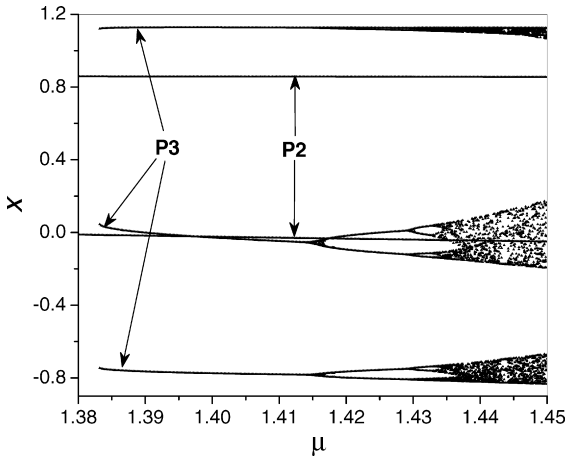

Fig. 2. Bifurcation diagram of the Hénon map Eq. (1) with μ as a control parameter for $J = 0.166$. The period-2^0 limit cycle coexists with the period-3^1 branch.

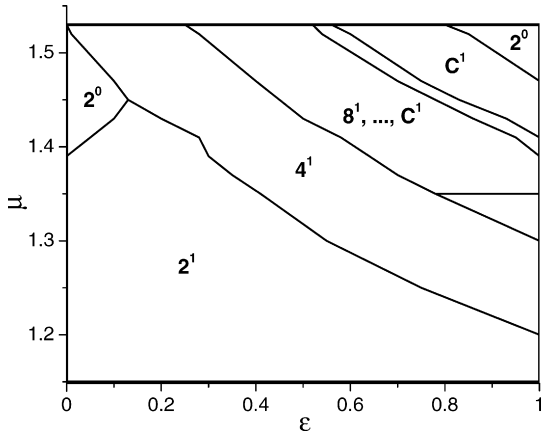

Fig. 3. State diagram of the slave system in the (ε,μ)-parameter space for $J = 0.166$. 2^1, 4^1, 8^1, and C^1 are the period-2, -4, -8 periodic and chaotic regimes which coexist with the period-2^0 regime of the master system.

periodic and chaotic regimes which coexist with the period 2^0 of the master system.

The bifurcation diagram of the slave map variable u with μ as a control parameter for $\varepsilon = 1$ is shown in Fig. 4 (red dots). In the same figure for reference we plot the bifurcation diagram of the master map variable x (blue dots). One can see that even for the total 100% coupling (at $\varepsilon = 1$ the variable v is substituted by the variable y), the slave map is still multistable. The attractor similar to that of the master map also exists; the maps are completely synchronized only if the slave map stays in the similar attractor.

2.2. Fixed points analysis

To find the difference in steady-state solutions of the solitary and the two coupled Hénon maps, we make the fixed point analysis. The characteristic equation for the master map Eq. (1) is $\mu x^2 + (J+1)x - 1 = 0$ and therefore it has two fixed points:

$$x^*_{1,2} = \frac{-(J+1) \pm \sqrt{(J+1)^2 + 4\mu}}{2\mu},$$
$$y^*_{1,2} = -J x^*_{1,2}. \tag{3}$$

For two coupled maps, using Eqs. (1) and (2) we get the characteristic equation $\mu u^2 + (J + 1 + \varepsilon J)u - (1 + \varepsilon y^*_{1,2}) = 0$ which yields four fixed points:

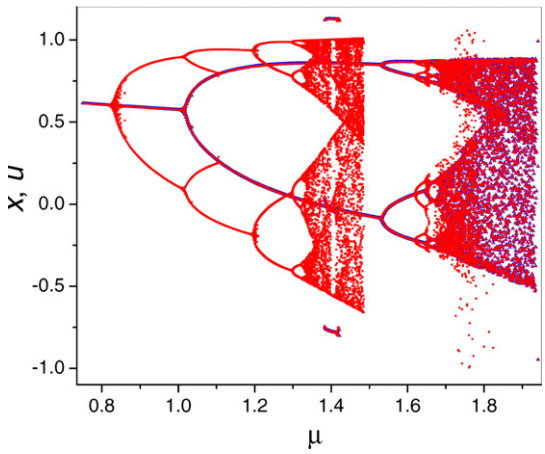

Fig. 4. Bifurcation diagram of the slave map (red dots) for $\varepsilon = 1$ and $J = 0.166$ with μ as a control parameter. Blue dots show the master map state which coexists in the slave map. The slave map is completely synchronized with the master map only if it stays in the similar attractor. (For interpretation of the references to color in this figure legend, the reader is referred to the web version of this Letter.)

$$u_k^* = \frac{-(J+1-\varepsilon J) \pm \sqrt{(J+1-\varepsilon J)^2 + 4\mu(1-\varepsilon J x_{1,2}^*)}}{2\mu},$$
$$v_k^* = -J u_k^*, \tag{4}$$

where $k = 1, 2, 3, 4$ is the fixed point number.

When the maps is completely coupled, i.e. $\varepsilon = 1$, the fixed points of the slave map are

$$\overline{u_k} = \frac{-1 \pm \sqrt{1 + 4\mu(1 - J x_{1,2}^*)}}{2\mu},$$
$$\overline{y_k} = -J\overline{u_k}. \tag{5}$$

By comparing Eqs. (3) and (5), one can see that the fixed points of the solitary and coupled maps are different even for 100% coupling, i.e. when one of the variables of the slave map is substituted by the variable of the master map in Eq. (2). This is the important difference from continuous time systems [10–13].

3. Coexistence of two different periodic orbits

In this section, we study synchronization of two identical Hénon maps in the range of the coexistence of two different periodic orbits, in particular, when the uncoupled maps ($\varepsilon = 0$) exhibit the coexistence of the period-2 and the period-3 orbits. This case occurs for the parameters $\mu = 1.4$ and $J = 0.166$ (see Fig. 2). Two different situations are possible: (i) the master map stays in the period 2 and (ii) the master maps stays in the period 3. In the following, we will analyze the bifurcation diagrams with respect to the coupling strength ε and measure the synchronization time as a function of ε.

3.1. Master in period 2, slave in period 3

First, we consider the situation when the master map stays in the period 2 and the slave map initially ($\varepsilon = 0$) stays in the period 3. Fig. 5(a) shows the bifurcation diagram of the slave map variable u with ε as a control parameter. One can see that the initial period-3 orbit exists in the slave system only for a very weak coupling strengths ($\varepsilon < 0.05$), and for a larger coupling this attractor disappears. Meanwhile two other attractors coexist, these are the period-2 orbit which coincides with the period-2 attractor of the master system ($u \equiv x$) and does not change with ε, and another different period-2 attractor which with increasing ε undergoes a cascade of period-doubling bifurcations leading to chaos.

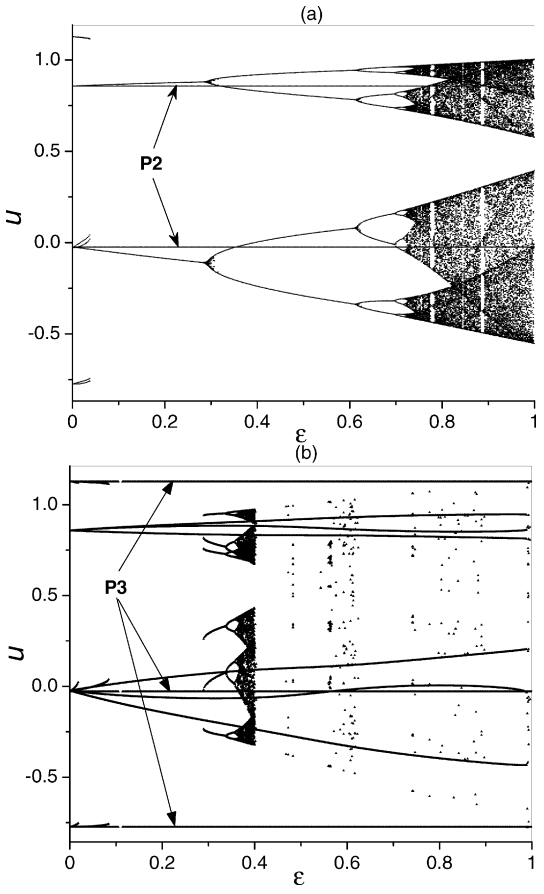

Fig. 5. Bifurcation diagram of slave map variable u with respect to coupling strength ε when (a) master map stays in period 2 and slave map initially stays in period 3 and (b) master map stays in period 3 and slave map initially stays in period 2. $\mu = 1.4$ and $J = 0.166$.

3.2. Master in period 3, slave in period 2

Another situation occurs when the master map is in the period 3 and the slave map initially stays in the period 2. The corresponding bifurcation diagram is shown in Fig. 5(b). As in the previous case, the initial attractor (period 2) exists only for a very low coupling strength ($\varepsilon < 0.01$), and the period-3 attractor of the master map always exists and does not change with ε. Meanwhile, a new period-6 attractor appears and changes when ε is increased. Moreover, another different period 6 arises in the saddle-node bifurcation at $\varepsilon \approx 0.27$ and undergoes a cascade of period-doubling bifurcations leading to chaos. Thus, for $\varepsilon > 0.27$ the slave map exhibits the coexistence of as many as three attractors.

The analysis of the bifurcation diagrams calculated for different parameters μ and J in the range of coexistence of different periodic regimes allows us to reveal the following main properties.

- The initial attractor of the slave map exists only for a very low coupling strength and disappears when the coupling strength is increased.
- The attractor of the master map always exists in the slave map independently of the coupling strength.
- The increasing coupling strength gives rise to new periodic orbits in the slave map which undergo period-doubling bifurcations leading to chaos.

3.3. Synchronization time

As was already mentioned above, the initial attractor of the slave system loses its stability at a certain critical coupling

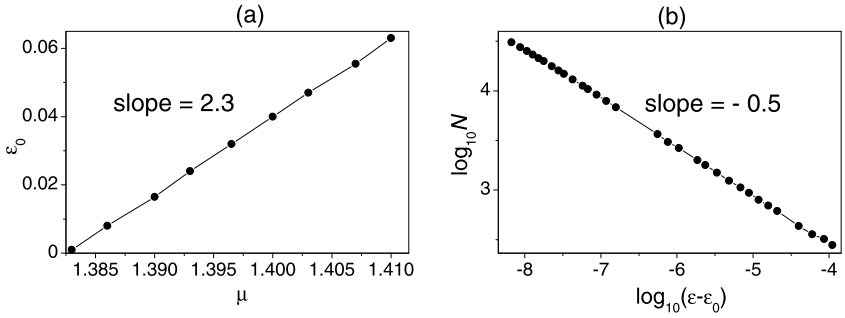

Fig. 6. (a) Critical coupling strength ε_0 at which the initial attractor of the slave map losses its stability, versus parameter μ. (b) Synchronization time (in number of iterations N) as a function of coupling strength in the log–log scale for $\mu = 1.4$ and $J = 0.166$. The master map is in the period 2, while the slave map initially stays in the period 3.

strength ε_0. We find that this value increases linearly as μ is increased, as shown in Fig. 6(a).

For $\varepsilon > \varepsilon_0$, the initial periodic orbit is observed only in transients after which the trajectory is attracted to the periodic orbit similar to that of the master map. In other words, the transient time is a time needed to synchronize the slave and the master maps towards the same periodic orbit. Fig. 6(b) shows how this synchronization time depends on the coupling strength. For small ε, we find that this dependence obeys a -0.50 ± 0.08 power law. It seams that this value is universal, because it is almost independent of μ and of the periodicity of master map attractor.

4. Coexistence of periodic and chaotic orbits

In this section, we will consider the coupled maps in the parameter region where the period 2 coexists with chaos, i.e. we explore the parameters $\mu = 1.45$ and $J = 0.166$ (see Fig. 2). Here, also two situations are possible: (i) the master map stays in the period 2 and (ii) the master map stays in chaos. In the following we will analyze both situations.

4.1. Master in period 2, slave in chaos

Fig. 7(a) shows the bifurcation diagram of the slave variable u with ε as a control parameter when the master map is in the period 2 and the slave map initially stays in chaos.

We see again that the master map attractor (period 2) always exists in the slave map and it does not change with ε, whereas the initial chaotic attractor undergoes inverse period-doubling bifurcations and disappears in crisis. Meanwhile, even a very small coupling gives rise to a different period-2 attractor which undergoes a cascade of period-doubling bifurcations terminated in chaos, as the coupling strength is increased.

4.2. Master in chaos, slave in period 2

The most complex dynamics is observed when the master map is in chaos, while the slave map initially stays in the period 2. The bifurcation diagram for this case is shown in Fig. 7(b). The slave map is always chaotic, including the coexistence of different chaotic attractors. It is remarkable, that for $\varepsilon > 0.6$ there are no empty spaces and periodic windows within a certain range of the variable, that makes this regime very prominent for chaotic cryptography [18].

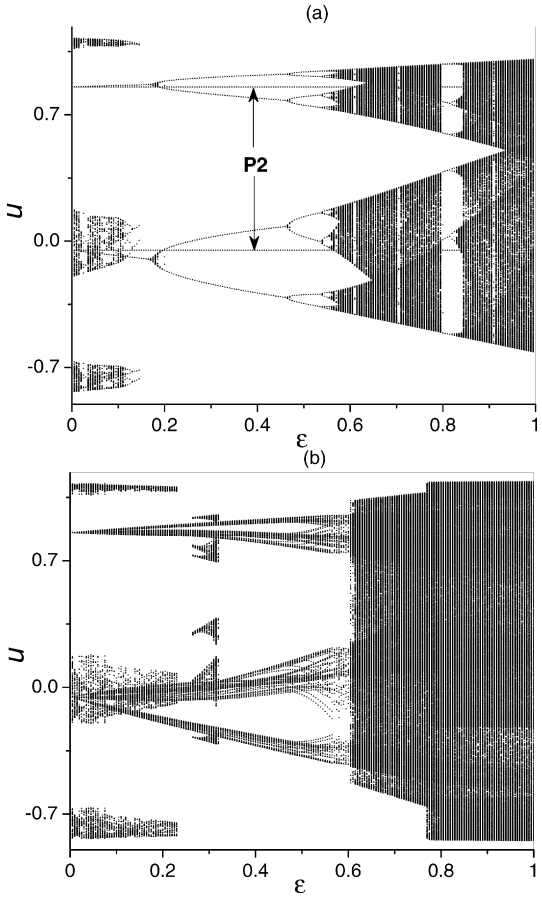

Fig. 7. Bifurcation diagram of slave map variable u with respect to coupling strength ε when (a) master map is in the period 2, while slave map initially stays in chaos and (b) master map is in chaos, while slave map initially stays in period 2. $\mu = 1.45$ and $J = 0.166$.

5. Conclusions

We have studied complex dynamics of two identical unidirectionally coupled Hénon maps with coexisting attractors. In particular, we explored the parameter ranges where the uncoupled maps exhibit the coexistence of different periodic attractors, and one periodic and one chaotic attractor. In the former case, the synchronization time obeys a $-1/2$ power law with respect to the coupling strength and is almost independent of the map parameters and of the periodicity of the periodic orbit. In the latter case, an increase in the coupling strength gives rise to new attractors resulting in multistability, including the coexistence of different chaotic attractors. For a high coupling strength, the slave map remains bistable and complete synchronization can be achieved only when the slave map stays in the similar attractor as the master map.

Given the importance, the Hénon map has held as the canonical models for simple systems that exhibit multistability, we believe

that the results of this work will have wider-reaching implications for investigation of more complex dynamical systems with coexisting attractors.

Acknowledgements

This work was supported by Consejo Nacional de Ciencia y Tecnologia of Mexico (projects Nos. 100429 and J49731).

References

[1] J. Maurer, A. Libchaber, J. Phys. Lett. 41 (1980) 515.
[2] E. Brun, B. Derighetti, D. Meier, R. Holzner, M. Raveni, J. Opt. Soc. Am. B 2 (1985) 156.
[3] J.M.T. Thompson, H.B. Stewart, Nonlinear Dynamics and Chaos, Wiley, Chichester, 1986.
[4] J. Foss, A. Longtin, B. Mensour, J. Milton, Phys. Rev. Lett. 76 (1996) 708.
[5] L. Poon, C. Grebogi, Phys. Rev. Lett. 75 (1995) 4023.
[6] U. Feudel, C. Grebogi, B.R. Hunt, J.A. Yorke, Phys. Rev. E 54 (1996) 71.
[7] U. Feudel, C. Grebogi, Chaos 7 (1997) 597.
[8] D.E. Postnov, T.E. Vadivasova, O.V. Sosnovtseva, A.G. Balanov, V.S. Anishchenko, E. Mosekilde, Chaos 9 (1999) 227.
[9] S. Yanchuk, T. Kapitaniak, Phys. Rev. E 64 (2001) 056235.
[10] A.N. Pisarchik, R. Jaimes-Reátegui, J.R. Villalobos-Salazar, J.H. García-Lopez, S. Boccaletti, Phys. Rev. Lett. 96 (2006) 244102.
[11] A.N. Pisarchik, R. Jaimes-Reátegui, J.H. García-Lopez, Int. J. Biffur. Chaos 18 (2008) 1801.
[12] A.N. Pisarchik, R. Jaimes-Reátegui, J.H. García-Lopez, Phil. Trans. Roy. Soc. A (London) 366 (2008) 459.
[13] F.R. Ruiz-Oliveras, A.N. Pisarchik, Phys. Rev. E 79 (2009) 016202.
[14] V. Astakhov, A. Shabunin, W. Uhm, S. Kim, Phys. Rev. E 63 (2001) 056212.
[15] W. Uhm, V. Astakhov, A. Akopov, S. Kim, Int. J. Mod. Phys. B 17 (2003) 4013.
[16] T. Kapitaniak, Phys. Rev. E 53 (1996) 6555.
[17] M. Henon, Commun. Math. Phys. 50 (1976) 69.
[18] A. Jolfaei, A. Mirghadri, International Review on Computers and Software 6 (2011) 40.